Properties of $Q\bar{Q}$ $(Q \epsilon b, c)$ mesons in Coulomb plus Power potential

Bhavin Patel and P.C.Vinodkumar

Department of Physics, Sardar Patel University, Vallabh Vidyanagar- 388 120, Gujarat, INDIA

E-mail: azadpatel2003@yahoo.co.in

Abstract. The decay rates and spectroscopy of the $Q\bar{Q}$ $(Q \in c, b)$ mesons are computed in non-relativistic phenomenological quark antiquark potential of the type $V(r) = -\frac{\alpha_c}{r} + Ar^{\nu}$, (CPP$_{\nu}$) with different choices ν. Numerical solution of the schrodinger equation has been used to obtain the spectroscopy of $Q\bar{Q}$ mesons. The spin hyperfine, spin-orbit and tensor components of the one gluon exchange interaction are employed to compute the spectroscopy of the few lower S and orbital excited states. The numerically obtained radial solutions are employed to obtain the decay constant, di-gamma and di-leptonic decay widths. The decay widths are determined with and without radiative corrections. Present results are compared with other potential model predictions as well as with the known experimental values.

PACS numbers: 12.39Jh, 12.40Yx, 13.20Gd

1. Introduction

Heavy flavour hadrons play an important role in several high energy experiments as well as in the understanding of the theories like QCD, NRQCD, pNRQCD, vNRQCD and effective field theories. The BES at the Beijing Electron Positron Collider (BEPC), E835 at Fermilab, and CLEO at the Cornell Electron Storage Ring (CESR) are able to collect the huge data on heavy flavour mesons. Where as B-meson factories, BaBar at PEP-II and Belle at KEKB are working on the observation of new and possibly exotics quarkonia states. The CDF and Dϕ experiments at Fermilab measuring heavy quarkonia production from gluon-gluon fusion in $p\bar{p}$ annihilations at 2 TeV. Also some other experiments like ZEUS and H1 at DESY are studying charmonia production in photon-gluon fusion. The study related to the charmonia production and suppression in heavy-ion collisions are being looked by PHENIX, STAR and NA60. All these experiments are capable of observing new states, new production mechanisms, new decays and transitions, and in general to the collection of high statistics and precision data sample. In the near future, even larger data samples are expected from the BES-III upgraded experiment, while the B factories and the Fermilab Tevatron will continue to supply valuable data for few years. Later on, the LHC experiments at CERN, Panda at GSI etc are capable of offering future opportunities and challenges in this field of heavy flavour physics [1].

On the theoretical side, heavy quarkonium provides testing and the validity of perturbative QCD, potential models and lattice QCD calculations [2]. The investigation of the properties of mesons composed of a heavy quark and antiquark ($c\bar{c}$, $b\bar{c}$, $b\bar{b}$) gives very important insight into heavy quark dynamics and to the understanding of the constituent quark masses. The theoretical predictions of the heavy quarkonia $c\bar{c}$, $b\bar{c}$ and $b\bar{b}$ mesons have rich spectroscopy with many narrow states of charmonium lying under the threshold of open charm production [3, 4] and of botomonium lying under the threshold of $B-B$ production. Many of these states have not confirmed or understood by experiments [5]. However, there have been renewed interest in the spectroscopy of the heavy flavoured hadrons due to number of experimental facilities (CLEO, DELPHI, Belle, BaBar, LHCb etc) which have been continuously providing and expected to provide more accurate and new informations about these states at the heavy flavour sector. At the hadronic scale the non-perturbative effects connected with complicated structure of QCD vacuum necessarily play an important role. All this leads to a theoretical uncertainty in the $Q\bar{Q}$ potential at large and intermediate distances. It is just in this region of large and intermediate distance that most of the basic hadron resonances are formed. So the success of theoretical model predictions of most of the hadronic properties with experiments can provide important information about the quark-antiquark interactions. Such information is of great interest, as it is not possible to obtain the $Q\bar{Q}$ potential starting from the basic principle of the quantum chromodynamics (QCD) at the hadronic scale.

Among many theoretical attempts or approaches to explain the hadron properties based

on its quark structure very few were successful in predicting the hadronic properties starting from its spectroscopy to decay rates. The nonrelativistic potential models with Buchmüller and Tye [6], Martin [7, 8, 9], Log [10, 11], Cornell [12] etc. were successful in predictions of the spectra of the heavy flavour mesons while the Bethe-Salpeter approach under harmonic confinement [13] were successful at low flavour sector. Though there exist relativistic approaches for the study of the different hadronic properties [14, 15, 16], the non-relativistic models have also been equally successful at the heavy flavour sector. For the theoretical predictions of different decay rates most of the models require supplementary corrections such as higher order QCD effects, radiative contributions etc. Even in some cases rescaling of the model radial wave functions are also being considered. However the NRQCD formalism provides a systematic approach to study the decay properties like the di-gamma and the di-lepton decays. These partial decay widths provide an account of the compactness of the qurkonium system which is an useful information complementary to spectroscopy [17]. Thus, in this paper we make an attempt to study the properties like mass spectrum, decay constants and other decay properties of the $Q\bar{Q}$ systems ($Q\ \epsilon\ b, c$) based on a phenomenological coulomb plus power potential (CPP$_\nu$). Here, we consider different choices of the potential power index ν to study the properties of the mesonic systems upto few excited states.

2. Nonrelativistic Treatment for Heavy Quarks

There are many theoretical approaches both relativistic and nonrelativistic to study the heavy quark systems [11, 18, 19, 20, 21, 22, 23, 24, 25, 26, 27, 28]. However their predictions suggests the successes of the nonrelativistic treatment for the heavy flavour quark-antiquark system [11]. The relativistic invariant theory for example light-front QCD [29] though deals with different aspects of QCD, under non-relativistic approximations, reproduces the results comparable to the non-relativistic quark-potential models [29]. In the center of mass frame of the heavy quark-antiquark system, the momenta of the quark and antiquark are dominated by their rest mass $m_{Q,\bar{Q}} \gg \Lambda_{QCD} \sim |\vec{p}\,|$, which constitutes the basis of the non-relativistic treatment. For examples NRQCD formalism for the heavy quarkonia, the velocity of heavy quark is chosen as the expansion parameter [30].
Hence, for the study of heavy-heavy bound state systems such as $c\bar{c}$, $b\bar{c}$ and $b\bar{b}$, we consider a nonrelativistic Hamiltonian given by [24, 25, 26]

$$H = M + \frac{p^2}{2M_1} + V(r) \tag{1}$$

where

$$M = m_Q + m_{\bar{Q}}, \quad \textit{and} \quad M_1 = \frac{m_Q\ m_{\bar{Q}}}{m_Q + m_{\bar{Q}}} \tag{2}$$

m_Q and $m_{\bar{Q}}$ are the mass parameters of quark and antiquark respectively, p is the relative momentum of each quark and $V(r)$ is the quark antiquark potential. Though linear plus

Table 1. The model Parameters employed in the present study: (The potential strength A for different power index, ν is given in $\mathrm{GeV}^{\nu+1}$)

ν	A $(c\bar{c})$	A $(b\bar{c})$	A $(b\bar{b})$
0.5	0.3630	0.4085	0.4600
0.7	0.3034	0.3582	0.4430
0.8	0.2784	0.3366	0.4358
0.9	0.2559	0.3169	0.4296
1.0	0.2355	0.2986	0.4237
1.1	0.2170	0.2817	0.4180
1.3	0.1846	0.2513	0.4080
1.5	0.1573	0.2246	0.3984

$\alpha_c(c\bar{c}) = 0.40$, $\alpha_c(b\bar{c}) = 0.34$, $\alpha_c(b\bar{b}) = 0.30$,
$m_c = 1.24\ GeV$ and $m_b = 4.50\ GeV$

coulomb potential is a successful well studied non-relativistic model for heavy flavour sector, their predictions for decay widths are not satisfactory owing to the improper value of the radial wave function at the origin compared to other models [25]. Thus, in the present study we consider a general power potential with color coulomb term of the form

$$V(r) = \frac{-\alpha_c}{r} + Ar^{\nu} \tag{3}$$

as the static quark-antiquark interaction potential. This potential belong to the special choices of the generality of the potentials, $V(r) = -Cr^{\alpha} + Dr^{\beta} + V_0$ [31, 32, 33] with $V_0 = 0$ $\alpha = -1$, $\beta = \nu$. For the present study, the power index range of $0.1 < \nu < 2.0$ have been explored. Here, for mesons, $\alpha_c = \frac{4}{3}\alpha_s$, α_s being the strong running coupling constant, A is the potential parameter similar to the string strength and ν is a general power, such that the choice, $\nu = 1$ corresponds to the coulomb plus linear potential. The different choices of ν here, correspond to different potential forms. In general, the potential parameter A can also be different numerically and dimensionally for each choices of ν. In the present study of heavy-heavy flavour mesons, we employ the numerical approach [34] to generate the Schrödinger mass spectra.

3. Spin-Dependent forces in $Q\bar{Q}$ States

In general, the quark-antiquark bound states are represented by $n^{2S+1}L_J$, identified with the J^{PC} values, with $\vec{J} = \vec{L} + \vec{S}$, $\vec{S} = \vec{S}_Q + \vec{S}_{\bar{Q}}$, parity $P = (-1)^{L+1}$ and the charge conjugation $C = (-1)^{L+S}$ with (n, L) being the radial quantum numbers. So the S-wave ($L = 0$) bound states are represented by $J^{PC} = 0^{-+}$ and 1^{--} respectively. The P-wave ($L = 1$) states are represented by $J^{PC} = 1^{+-}$ with $L = 1$ and $S = 0$ while $J^{PC} = 0^{++}$, 1^{++} and 2^{++} correspond to $L = 1$ and $S = 1$ respectively. Accordingly,

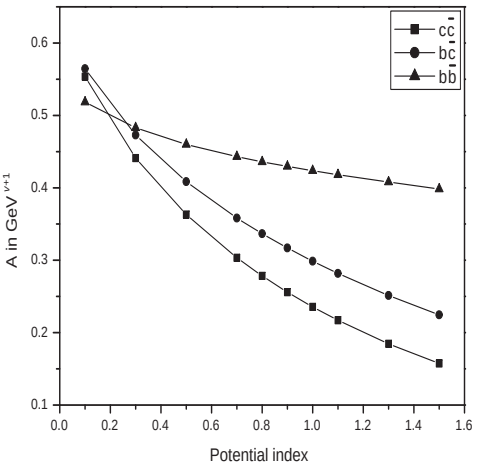

Figure 1. Behavior of A with the potential index ν for different $Q\bar{Q}$ systems

the spin-spin interaction among the constituent quarks provides the mass splitting of $J = 0^{-+}$ and 1^{--} states, while the spin-orbit interaction provides the mass splitting of $J^{PC} = 0^{++},\ 1^{++}$ and 2^{++} states. The $J^{PC} = 1^{+-}$ state with $L = 1$ and $S = 0$ represents the center of weight mass of the P-state as its spin-orbit contribution becomes zero, while the two $J = 1^{+-}$ singlet and the $J = 1^{++}$ of the triplet P-states form a mixed state. The D-wave ($L = 2$) states are represented by $J^{PC} = 2^{-+}$ with $L = 1$ and $S = 0$ while $J^{PC} = 3^{--},\ 2^{-+}$ and 1^{-+} correspond to $L = 2$ and $S = 1$ respectively.

For computing the mass difference between these states, we consider the spin dependent part of the usual OGEP given by [35] as

$$V_{S_{\bar{Q}}\cdot S_Q}(r) = \frac{2}{3}\frac{\alpha_c}{M_{\bar{Q}}m_Q}\ \vec{S_{\bar{Q}}}\cdot\vec{S_Q}\ 4\pi\delta(\vec{r});\quad V_{L\cdot S}(r) = \frac{\alpha_c}{M_{\bar{Q}}m_Q}\ \frac{\vec{L}\cdot\vec{S}}{r^3} \tag{4}$$

and

$$V_T(r) = \frac{\alpha_c}{M_{\bar{Q}}m_Q}\ \frac{(3(\vec{S}\cdot\vec{n})(\vec{S}\cdot\vec{n}) - \vec{S}\cdot\vec{S})}{r^3},\quad \vec{n} = \frac{\vec{r}}{r} \tag{5}$$

The spin average mass for the ground state is computed for the different choices of ν in the range, $0.5 < \nu < 1.5$. The model parameters used here are listed in Table 1. The potential parameter A are fixed for each choices of ν so as to get the experimental ground state spin average masses of $Q\bar{Q}$ systems. The spin average masses of $c\bar{c}$ is computed using the experimental ground state mass of $M_{\eta_c} = 2.980$ GeV and $M_{J/\psi} = 3.097$ GeV [5], while the experimental values of $M_\Upsilon = 9.460$ GeV and theoretically predicted values for η_b, $M_{\eta_b} = 9.400$ GeV [15] are used to get the centre of weight mass of $b\bar{b}$ system. For the $b\bar{c}$ meson we use the experimental mass of $M_{B_c} = 6.286$ GeV [5] and the theoretically predicted value of $M_{B_c^*} = 6.332$ GeV [15]. For the nJ state, we compute the spin-average or the center of weight mass from the respective experimental

values as

$$M_{CW,n} = \frac{\sum_J 2(2J+1)\ M_{nJ}}{\sum_J 2(2J+1)} \tag{6}$$

In the case of quarkonia ($c\bar{c}$ and $b\bar{b}$ systems)many orbital excited states are known. Theoretical predictions of all these states and their decay widths are also being studied. But in many cases, the decay widths and the spin splitting between different J values are not well reproduced. Both the decay widths and the level splitting of the spectra due to the one gluon exchange interaction terms are related to the values of the radial wave function or its derivatives at the origin. Thus, the inappropriate description of the $Q\bar{Q}$ radial wave function led to the disparity among the different model predictions of the decay widths and level splitting. In some cases, for better predictions of the excited spectra of quarkonia, the strong running coupling constant α_s are evaluated interms of the average kinetic energy of the quark-antiquark pair at a given state. Accordingly, different excited states corresponds to have different values of α_s [35, 36]. However, the radial wave functions are found to be less sensitive to the changes in α_s compared to similar changes in the values of the strength of the confining part of the potential. Hence, in this paper, we allow A to vary mildly with radial quantum number ($n = 0, 1, 2...$) as $A = \frac{A}{(n+1)^{\frac{1}{4}}}$. The variation in A can be justified by similar arguments for the changes in α_S with the average kinetic energy. Here, as the system get excited, the average kinetic energy increases and hence the potential strength (the spring tension) reduces. With this mild state dependence on the potential parameter A, we obtain the excited spectra as well as the right behavior for the radial wave functions . The computed values of the radial wave function at the origin for $(n+1)S$ states are listed in Table 2 for all the $Q\bar{Q}$ combinations. Using the spin dependent potential given by Eqn. 4 and 5, we compute the masses of the different $n^{2S+1}L_J$ states of $c\bar{c}$, $b\bar{c}$ and $b\bar{b}$ mesons. Better stastics with respect to the experimental values are observed with our predictions of these states for the potential index lying between 0.7 to 1.3. Thus we list our predicted properties in this range of potential index only. The computed masses of the $Q\bar{Q}$ mesonic states are listed in Table 3 in the case of $c\bar{c}$, in Table 4 in the case of $b\bar{c}$ and in Table 5 in the case of $b\bar{b}$ systems along with the available experimental values as well as other model predictions. Fig 1 shows the behavior of A with the potential index ν that provide us the ground state center of weight masses for all the three ($c\bar{c}$, $b\bar{c}$ and $b\bar{b}$) combinations of $Q\bar{Q}$ systems.

4. The Decay constants of the heavy flavoured mesons

The decay constants of mesons are important parameters in the study of leptonic or non-leptonic weak decay processes. The decay constants of pseudoscalar (f_P) and vector (f_V) states are obtained by prarameterizing the matrix elements of weak current between the corresponding mesons and the vacuum as

$$\langle 0|\bar{Q}\gamma^{\mu}\gamma_5 Q|P_{\mu}(k)\rangle = if_P k^{\mu} \tag{7}$$

Table 2. The radial Wave function $|R_{ns}(0)|^2$ (in GeV^3) of $Q\bar{Q}$ systems in various potential models including CPP$_\nu$.

Mesonic System	Potential Model	$1S$	$2S$	$3S$	$4S$	$5S$	$6S$
$c\bar{c}$	(CPP$_\nu$), $\nu = 0.5$	0.420	0.198	0.136	0.106	0.088	0.075
	0.7	0.529	0.295	0.221	0.182	0.158	0.141
	0.8	0.577	0.347	0.270	0.229	0.202	0.183
	0.9	0.622	0.400	0.323	0.280	0.252	0.232
	1.0	0.662	0.454	0.379	0.337	0.309	0.288
	1.1	0.700	0.509	0.439	0.399	0.372	0.352
	1.3	0.767	0.623	0.569	0.538	0.517	0.502
	Martin [7]	0.979	0.545	0.390	0.309	0.257	0.222
	Log [10]	0.796	0.406	0.277	0.211	0.172	0.145
	Cornell [37]	1.458	0.930	0.793	0.725	0.683	0.654
	Buchmuller-Tye [6]	0.794	0.517	0.441	0.404	0.381	0.365
	Lichtenberg-Wills [38]	1.121	0.693	0.563	0.496	0.453	0.423
$b\bar{c}$	(CPP$_\nu$), $\nu = 0.5$	0.886	0.411	0.280	0.217	6.865	0.154
	0.7	1.109	0.609	0.454	0.373	7.221	0.288
	0.8	1.207	0.714	0.553	0.468	7.414	0.374
	0.9	1.298	0.823	0.661	0.573	7.615	0.473
	1.0	1.381	0.933	0.776	0.688	7.823	0.587
	1.1	1.457	1.047	0.898	0.814	8.039	0.716
	1.3	1.594	1.278	1.163	1.098	8.487	1.020
	Martin [7]	1.720	0.957	0.685	0.452	0.452	0.390
	Log [10]	1.508	0.770	0.524	0.401	0.325	0.275
	Cornell [37]	3.191	1.769	1.449	1.297	1.205	1.141
	Buchmuller-Tye [6]	1.603	0.953	0.785	0.705	0.658	0.625
	Lichtenberg-Wills [38]	2.128	1.231	0.975	0.846	0.766	0.711
$b\bar{b}$	(CPP$_\nu$), $\nu = 0.5$	4.222	1.750	1.151	0.876	0.716	0.610
	0.7	5.101	2.534	1.828	1.479	1.265	1.118
	0.8	5.487	2.948	2.214	1.840	1.607	1.443
	0.9	5.843	3.377	2.632	2.244	1.996	1.820
	1.0	6.170	3.814	3.078	2.687	2.433	2.251
	1.1	6.470	4.259	3.551	3.168	2.917	2.735
	1.3	7.006	5.173	4.575	4.249	4.034	3.877
	Martin [7]	4.423	2.461	1.763	1.394	1.164	1.004
	Log [10]	4.706	2.401	1.636	1.250	1.015	0.857
	Cornell [37]	14.060	5.681	1.449	3.672	3.322	3.088
	Buchmuller-Tye [6]	6.253	3.068	2.356	2.032	1.845	1.721
	Lichtenberg-Wills [38]	6.662	3.370	2.535	2.139	1.902	1.740

Table 3. Mass spectra (in GeV) of $c\bar{c}$ states.

Meson	**Potential index ν**						Expt.	EFG03	ZVR95	BGE05
State	0.7	0.8	0.9	1.0	1.1	1.3	[5]	[15]	[39]	[3]
1^3S_1	3.091	3.093	3.095	3.097	3.099	3.101	3.097	3.096	3.100	3.090
1^1S_0	2.999	2.993	2.987	2.982	2.977	2.968	2.980	2.979	3.000	2.982
1^3P_2	3.450	3.488	3.523	3.557	3.589	3.647	3.556	3.556	3.540	3.556
1^3P_1	3.419	3.451	3.481	3.508	3.535	3.582	3.511	3.510	3.500	3.505
1^3P_0	3.403	3.432	3.459	3.484	3.508	3.549	3.415	3.424	3.440	3.424
1^1P_1	3.434	3.469	3.502	3.533	3.562	3.614		3.526	3.510	3.516
2^3S_1	3.457	3.519	3.580	3.641	3.700	3.815	3.686	3.686	3.730	3.672
2^1S_0	3.406	3.459	3.511	3.562	3.611	3.707	3.654	3.588	3.670	3.630
1^3D_3	3.683	3.751	3.817	3.879	3.939	4.051		3.815	3.830	3.806
1^3D_2	3.694	3.764	3.832	3.898	3.960	4.078		3.813	3.820	3.800
1^3D_1	3.677	3.744	3.808	3.869	3.927	4.036	3.770	3.798	3.800	3.785
1^1D_2	3.686	3.754	3.820	3.883	3.944	4.057		3.811	3.820	3.799
2^3P_2	3.662	3.755	3.847	3.939	4.030	4.209		3.972	4.020	3.972
2^3P_1	3.639	3.727	3.814	3.900	3.985	4.150		3.929	3.990	3.925
2^3P_0	3.628	3.713	3.797	3.880	3.962	4.120		3.824	3.940	3.852
2^1P_1	3.651	3.741	3.831	3.919	4.007	4.179		3.945	3.990	3.954
3^3S_1	3.673	3.784	3.897	4.011	4.125	4.355	4.040	4.088	4.180	4.072
3^1S_0	3.635	3.737	3.841	3.945	4.049	4.256		3.991	4.130	4.063
4^3S_1	3.833	3.987	4.146	4.309	4.475	4.816	4.415			4.406
4^1S_0	3.801	3.947	4.097	4.250	4.406	4.723				4.384
5^3S_1	3.962	4.155	4.356	4.564	4.780	5.229				
5^1S_0	3.935	4.120	4.312	4.511	4.716	5.140				
6^3S_1	4.073	4.300	4.540	4.792	5.055	5.609				
6^1S_0	4.049	4.269	4.500	4.742	4.994	5.522				

Table 4. Mass spactra (in GeV) of $b\bar{c}$ states.

Meson	**Potential index ν**						AEH05	EFG03	ZVR95
State	0.7	0.8	0.9	1.0	1.1	1.3	[40]	[15]	[39]
1^3S_1	6.328	6.329	6.330	6.331	6.332	6.333	6.416	6.332	6.340
1^1S_0	6.283	6.280	6.278	6.275	6.273	6.269	6.380	6.270	6.260
1^3P_2	6.700	6.737	6.772	6.804	6.835	6.891	6.837	6.762	6.760
1^3P_1	6.685	6.719	6.752	6.781	6.809	6.860	6.772	6.749	6.740
1^3P_0	6.678	6.711	6.741	6.770	6.797	6.845	6.693	6.734	6.730
1^1P_1	6.693	6.728	6.762	6.793	6.822	6.876	6.775	6.699	6.680
2^3S_1	6.709	6.770	6.831	6.890	6.949	7.063	6.896	6.881	6.900
2^1S_0	6.684	6.741	6.798	6.852	6.906	7.011	6.875	6.835	6.850
1^3D_3	6.947	7.016	7.083	7.146	7.208	7.322	7.003	7.081	7.040
1^3D_2	6.952	7.022	7.090	7.155	7.218	7.335	7.000	7.079	7.030
1^3D_1	6.944	7.013	7.079	7.142	7.202	7.315	6.959	7.077	7.020
1^1D_2	6.948	7.017	7.085	7.148	7.210	7.325	7.001	7.022	7.010
2^3P_2	6.918	7.011	7.103	7.194	7.285	7.462	7.186	7.156	7.160
2^3P_1	6.908	6.998	7.087	7.176	7.263	7.435	7.136	7.145	7.150
2^3P_0	6.902	6.991	7.080	7.166	7.252	7.421	7.081	7.126	7.140
2^1P_1	6.913	7.004	7.095	7.185	7.274	7.448	7.139	7.091	7.100
3^3S_1	6.930	7.041	7.154	7.268	7.382	7.611	7.215	7.235	7.280
3^1S_0	6.911	7.019	7.127	7.236	7.345	7.564	7.198	7.193	7.240
4^3S_1	7.093	7.247	7.407	7.570	7.737	8.079	7.468		
4^1S_0	7.077	7.228	7.384	7.542	7.704	8.035	7.452		
5^3S_1	7.224	7.418	7.620	7.829	8.046	8.498			
5^1S_0	7.211	7.401	7.599	7.804	8.015	8.455			
6^3S_1	7.337	7.565	7.807	8.060	8.324	8.883			
6^1S_0	7.325	7.550	7.788	8.036	8.295	8.841			

M(1^1S_0)=6.286 Expt. [5].

Table 5. Mass spectra (in GeV) of $b\bar{b}$ states.

Meson	**Potential index ν**						Expt.	EFG03	ZVR95
State	0.7	0.8	0.9	1.0	1.1	1.3	[5]	[15]	[39]
1^3S_1	9.458	9.459	9.460	9.460	9.461	9.463	9.460	9.460	9.460
1^1S_0	9.407	9.404	9.402	9.400	9.397	9.393		9.400	9.410
1^3P_2	9.855	9.891	9.926	9.958	9.989	10.046	9.913	9.913	9.860
1^3P_1	9.841	9.876	9.908	9.938	9.967	10.019	9.893	9.892	9.870
1^3P_0	9.835	9.868	9.899	9.928	9.955	10.006	9.860	9.863	9.850
1^1P_1	9.848	9.883	9.917	9.948	9.978	10.033		9.901	9.880
2^3S_1	9.861	9.920	9.979	10.037	10.094	10.205	10.023	10.023	10.020
2^1S_0	9.836	9.891	9.946	9.999	10.052	10.154		9.993	10.000
1^3D_3	10.102	10.171	10.238	10.302	10.363	10.479		10.162	10.150
1^3D_2	10.106	10.176	10.244	10.309	10.371	10.489	10.162	10.158	10.150
1^3D_1	10.099	10.168	10.234	10.298	10.358	10.473		10.153	10.140
1^1D_2	10.103	10.172	10.239	10.303	10.365	10.481		10.158	10.150
2^3P_2	10.075	10.165	10.256	10.346	10.435	10.611	10.269	10.268	10.280
2^3P_1	10.066	10.154	10.242	10.330	10.416	10.587	10.255	10.255	10.260
2^3P_0	10.061	10.148	10.236	10.322	10.407	10.575	10.232	10.234	10.240
2^1P_1	10.070	10.160	10.249	10.338	10.425	10.599		10.261	10.270
3^3S_1	10.083	10.191	10.301	10.412	10.523	10.748	10.355	10.238	10.290
3^1S_0	10.065	10.169	10.275	10.381	10.488	10.703		10.355	10.370
4^3S_1	10.244	10.394	10.549	10.709	10.871	11.207	10.279		
4^1S_0	10.229	10.375	10.527	10.682	10.840	11.165			
5^3S_1	10.373	10.560	10.757	10.961	11.173	11.616	10.865		
5^1S_0	10.360	10.544	10.737	10.937	11.144	11.576			
6^3S_1	10.482	10.703	10.938	11.185	11.443	11.991	11.019		
6^1S_0	10.471	10.688	10.920	11.163	11.416	11.952			

$$\langle 0|\bar{Q}\gamma^{\mu}Q|V(k,\epsilon)\rangle = f_V M_V \epsilon^{\mu} \tag{8}$$

where k is the meson momentum, ϵ^{μ} and M_V are the polarization vector and mass of the vector meson. In the non relativistic quark model, the decay constant can be expressed through the ground state wave function at the origin $\psi_{P,V}(0)$ by the Van-Royen-Weisskopf formula [41]. The value of the radial wave function for $0^{-\,+}, (R_P)$ and for $1^{--}, (R_V)$ states would be different due to their spin dependent hyperfine interaction. The spin hyperfine interaction of the heavy flavour mesons are small and this can cause a small shift in the value of the wave function at the origin. Though, many models neglect this difference between (R_P) and (R_V) we account this correction by considering

$$R_{nJ}(0) = R(0)\left[1 + (SF)_J \frac{< \varepsilon_{SD} >_{nJ}}{M_1}\right] \tag{9}$$

Where $(SF)_J$ and $< \varepsilon_{SD} >_{nJ}$ is the spin factor and spin interaction energy of the meson in the nJ state, while $R(0)$ and M_1 correspond to the radial wave function at the zero separation and reduced mass of the $Q\bar{Q}$ system. It can easily be seen that this expression is consistent with the relation

$$R(0) = \frac{3R_V + R_P}{4} \tag{10}$$

given by [42].Though most of the models predict the mesonic mass spectrum successfully, there are disagreements in the predictions of their decay constants. For example, the ratio $\frac{f_P}{f_V}$ was predicted to be > 1 as $m_P < m_V$ and their wave function at the origin $R_P(0) \sim R_V(0)$ by most of the cases [43]. The ratio computed in the relativistic methods [44] predicted the ratio $\frac{f_P}{f_V} < 1$, particularly in the heavy flavour sector. The disparity of the predictions of these decay constants play decisive role in the precision measurements of the weak decay parameters as well as the spectroscopic hyperfine splitting. So, we reexamine the predictions of the decay constants under different potential (by the choices of different ν) schemes employed in the present work. Incorporating a first order QCD correction factor, we compute,

$$f^2_{P/V} = \frac{3\left|R_{nS}(0)\right|^2}{\pi M_{P/V}} \bar{C}^2(\alpha_s) \tag{11}$$

here, $\bar{C}^2(\alpha_s)$ is the QCD correction factor given by [45]

$$\bar{C}^2(\alpha_s) = 1 + \frac{\alpha_s}{\pi}\left[\frac{m_Q - m_q}{m_Q + m_q}\; ln\frac{m_Q}{m_q} - \delta^{V,P}\right] \tag{12}$$

Where $\delta^V = \frac{8}{3}$ and $\delta^P = 2$. In the case of $c\bar{c}$ and $b\bar{b}$ systems, $\bar{C}^2(\alpha_s)$ becomes $1 - \frac{\alpha_s}{\pi}\delta^{V,P}$ as the first term within the square bracket vanishes. Our computed values of f_P and f_V without this correction and with the correction shown in brackets up to $6S$ states are tabulated in Tables 6 -8 along with available experimental results and with other theoretical predictions in the cases of $c\bar{c}$, $b\bar{c}$ and $b\bar{b}$ systems respectively.

Table 6. Pseudoscalar meson decay constant f_P (MeV), Vector meson decay constant f_V (MeV) and f_P/f_V of $c\bar{c}$ states (The bracketed quantities are with QCD corrections).

	CPP$_\nu$	1S	2S	3S	4S	5S	6S
f_P	0.7	365(295)	270(218)	230(186)	206(167)	189(153)	177(143)
	0.8	377(305)	287(232)	248(200)	224(181)	207(168)	195(157)
	0.9	388(314)	302(244)	264(214)	241(195)	224(181)	211(171)
	1.0	397(321)	316(255)	279(226)	256(207)	239(193)	226(183)
	1.1	404(327)	328(265)	292(236)	269(218)	253(205)	240(194)
	1.3	417(337)	348(282)	315(255)	293(237)	276(224)	264(213)
	[46]	335±75					
	[47]	292±25					
f_V	0.7	419(313)	291(217)	243(181)	216(161)	197(147)	184(137)
	0.8	439(327)	314(234)	266(198)	238(177)	219(163)	204(152)
	0.9	457(341)	336(250)	287(214)	259(193)	239(178)	225(167)
	1.0	473(352)	356(265)	308(230)	280(209)	260(194)	245(182)
	1.1	487(363)	375(280)	329(245)	300(224)	280(208)	264(197)
	1.3	512(382)	412(307)	367(274)	339(253)	318(237)	303(226)
	[5]	416±6	304±4	187±8	161±10		
	[47]	459±28					
	[44]	459±28	364±24	319±22	288±18	265±16	
	[16]	551	401				
$\frac{f_P}{f_V}$	0.7	0.87(0.94)	0.93(1.00)	0.95(1.03)	0.95(1.04)	0.96(1.04)	0.96(1.04)
	0.8	0.86(0.93)	0.91(0.99)	0.93(1.01)	0.94(1.02)	0.95(1.03)	0.96(1.03)
	0.9	0.85(0.92)	0.90(0.98)	0.92(1.00)	0.93(1.01)	0.94(1.02)	0.94(1.02)
	1.0	0.84(0.91)	0.89(0.96)	0.91(0.98)	0.91(0.99)	0.92(0.99)	0.92(1.01)
	1.1	0.83(0.90)	0.87(0.95)	0.89(0.96)	0.90(0.97)	0.90(0.99)	0.91(0.98)
	1.3	0.81(0.88)	0.84(0.92)	0.86(0.93)	0.86 (0.94)	0.87(0.95)	0.87(0.94)
	[5]	0.81±0.19					

[5] → PDG-2006, [46]→ Edwards-2001, [47]→ Cvetic-2004,
[44] → Wang-2006, [16]→Ebert-2003.

5. Mean Square Radii and Average quark Velocity of $Q\bar{Q}$ $(Q\epsilon b, c)$ mesons

Apart from the decay constants, $f_{P/V}$, other important properties associated with a mesonic state are the mean square radii $\langle r^2 \rangle$ and the mean square velocity of the quark/antiquark $\langle v_q^2 \rangle$. The mean square size of the mesonic states is an important in the estimations of hadronic transition widths [48, 49, 50] of different $Q\bar{Q}'$ systems. The average velocity of the quark and the antiquark within a $Q\bar{Q}$ bound state are important for the estimation of relativistic corrections and are useful particularly in the NRQCD formalism as well as in the estimation of the quarkonium production rates [51].

Table 7. Pseudoscalar meson decay constant f_P (MeV), Vector meson decay constant f_V (MeV) and f_P/f_V of $b\bar{c}$ states (The bracketed quantities are with QCD corrections).

	CPP$_\nu$	1S	2S	3S	4S	5S	6S
f_P	0.7	396(355)	289(260)	247(221)	222(199)	205(184)	192(172)
	0.8	412(370)	311(279)	270(242)	245(220)	228(204)	215(193)
	0.9	426(382)	331(297)	291(261)	267(240)	250(225)	237(213)
	1.0	439(393)	350(314)	312(280)	289(259)	272(244)	259(233)
	1.1	450(403)	368(330)	332(298)	310(278)	293(263)	281(252)
	1.3	468(420)	401(359)	369(331)	349(313)	334(299)	321(288)
	[15]	433					
	[35]	460±60					
	[52]	500					
f_V	0.7	414 (349)	296(250)	251(212)	225(190)	207(175)	194(164)
	0.8	432 (364)	320(270)	276(232)	249(210)	231(195)	218(184)
	0.9	448 (378)	342(288)	299(252)	273(230)	255(215)	242(204)
	1.0	463 (390)	363(306)	322(271)	297(250)	279(235)	265(224)
	1.1	476 (401)	383(323)	344(290)	320(270)	302(255)	289(243)
	1.3	498 (420)	421(355)	387(326)	364(307)	348(293)	335(282)
	[15]	503					
	[35]	460±60					
	[52]	500					
$\frac{f_P}{f_V}$	0.7	0.96(1.02)	0.98(1.04)	0.98(1.04)	0.99(1.05)	0.99(1.05)	0.99(1.05)
	0.8	0.95(1.02)	0.97(1.03)	0.98(1.04)	0.98(1.05)	0.99(1.05)	0.99(1.05)
	0.9	0.95(1.01)	0.97(1.03)	0.97(1.04)	0.98(1.04)	0.98(1.05)	0.98(1.04)
	1.0	0.95(1.01)	0.96(1.03)	0.97(1.03)	0.97(1.04)	0.97(1.04)	0.98(1.04)
	1.1	0.95(1.00)	0.96(1.02)	0.97(1.03)	0.97(1.03)	0.97(1.03)	0.97(1.04)
	1.3	0.94(1.00)	0.95(1.01)	0.95(1.02)	0.96(1.02)	0.96(1.02)	0.96(1.02)
	[15]	0.86					
	[35]	1.00					
	[52]	1.00					

[15]→ Ebert-2003, [35] → Gerstein-1995, [52]→ Eichten-1994.

We compute the mean square radii as

$$\langle r^2 \rangle = \int_0^\infty r^4 |R_{nl}(r)|^2 dr \tag{13}$$

and the average mean square quark/antiquark velocity for the $c\bar{c}$ and $b\bar{b}$ systems, according to the relation given by [53]

$$\langle (v_q)^2 \rangle = \frac{1}{2M_1}(E - \langle V(r) \rangle) \tag{14}$$

Here, E is the binding energy of the system, M_1 is the reduced mass of the mesonic system and $\langle V(r) \rangle$ is the expectation value of the potential. In the $b\bar{c}$ case, the velocity

Table 8. Pseudoscalar meson decay constant f_P (MeV), Vector meson decay constant f_V (MeV) and f_P/f_V of $b\bar{b}$ states (The bracketed quantities are with QCD corrections).

	CPP$_\nu$	1S	2S	3S	4S	5S	6S
f_P	0.7	708(606)	492(421)	414(355)	370(317)	340(291)	318(273)
	0.8	733(628)	528(453)	453(388)	409(350)	379(325)	357(306)
	0.9	756(647)	563(482)	490(420)	448(384)	419(359)	397(340)
	1.0	776(665)	596(511)	527(451)	486(416)	457(392)	436(373)
	1.1	794(680)	627(537)	562(481)	523(448)	495(424)	474(406)
	1.3	824(706)	686(587)	629(539)	594(509)	569(488)	549(471)
f_V	0.7	722(584)	497(402)	417(337)	372(301)	342(276)	320(259)
	0.8	749(606)	534(432)	457(369)	412(333)	382(309)	359(291)
	0.9	773(625)	571(462)	495(401)	452(365)	422(341)	399(323)
	1.0	795(643)	605(489)	533(431)	491(397)	462(373)	439(356)
	1.1	814(658)	638(516)	570(461)	529(428)	501(405)	479(388)
	1.3	847(685)	700(566)	641(518)	605(489)	578(468)	558(451)
	[5]	715±5	498±5	430±4	336±18	369±42	240±28
	[16]	839	562				
	[44]	498±20	366±27	304±27	259±22	228±16	
$\frac{f_P}{f_V}$	0.7	0.98(1.04)	0.99(1.05)	0.99(1.05)	0.99(1.05)	0.99(1.05)	0.99(1.05)
	0.8	0.98(1.04)	0.99(1.05)	0.99(1.05)	0.99(1.05)	0.99(1.05)	0.99(1.05)
	0.9	0.98(1.04)	0.99(1.04)	0.99(1.05)	0.99(1.05)	0.99(1.05)	0.99(1.05)
	1.0	0.98(1.03)	0.99(1.04)	0.99(1.05)	0.99(1.05)	0.99(1.05)	0.99(1.05)
	1.1	0.98(1.03)	0.98(1.04)	0.99(1.04)	0.99(1.05)	0.99(1.05)	0.99(1.05)
	1.3	0.97(1.03)	0.98(1.04)	0.98(1.04)	0.98(1.04)	0.98(1.04)	0.98(1.04)

[5] → PDG-2006, [44]→Wang-2006, [16]→ Ebert-2003.

of b and c quarks are obtained as

$$\langle (v_b)^2 \rangle = (E - \langle V(r) \rangle) \frac{2\ m_c}{m_b\ (m_b + m_c)} \tag{15}$$

$$\langle (v_c)^2 \rangle = (E - \langle V(r) \rangle) \frac{2\ m_b}{m_c\ (m_b + m_c)} \tag{16}$$

The computed rms radii up to $6S$ states of $c\bar{c}$, $b\bar{c}$ and $b\bar{b}$ systems are listed in Table 9 for the range of potential index $0.7 \leq \nu \leq 1.3$. The estimated rms velocity $\left\langle v_q^2 \right\rangle^{\frac{1}{2}}$ of the charm and beauty quark/antiquark using Eqn. 14 to 16 are given in Table 10 of $c\bar{c}$, $b\bar{c}$ and $b\bar{b}$ systems in their $1S$, $1P$, $1D$ and $2S$ to $6S$ states.

6. Decay rates of quarkonia

The spectroscopic parameters including the predicted masses and the resultant radial wave functions are being used here to compute the decay rates. We consider the

Table 9. Mean Square radii (fm) for the $Q\bar{Q}$ (Q ϵ b, c) states in various potential power index, ν.

	CPP$_\nu$ ν	1S	1P	2S	1D	2P	3S	4S	5S	6S
$c\bar{c}$	0.7	0.50	0.79	1.07	1.03	1.33	1.59	2.08	2.55	3.00
	0.8	0.48	0.74	0.99	0.96	1.23	1.46	1.89	2.30	2.69
	0.9	0.46	0.70	0.94	0.90	1.14	1.35	1.74	2.10	2.44
	1.0	0.45	0.67	0.89	0.85	1.07	1.26	1.61	1.93	2.23
	1.1	0.43	0.64	0.84	0.81	1.01	1.19	1.50	1.79	2.06
	1.3	0.41	0.59	0.77	0.74	0.92	1.07	1.33	1.56	1.79
	[23]	0.39		0.82			1.44	2.36		
	[54]	0.43		0.85			1.18	1.47		
$b\bar{c}$	0.7	0.39	0.62	0.84	0.82	1.06	1.26	1.65	2.02	2.38
	0.8	0.38	0.58	0.79	0.76	0.97	1.16	1.50	1.83	2.14
	0.9	0.36	0.55	0.74	0.71	0.91	1.07	1.38	1.67	1.94
	1.0	0.35	0.53	0.70	0.67	0.85	1.00	1.28	1.53	1.78
	1.1	0.34	0.51	0.67	0.64	0.80	0.94	1.19	1.42	1.64
	1.3	0.33	0.47	0.61	0.59	0.73	0.85	1.05	1.24	1.42
$b\bar{b}$	0.7	0.25	0.41	0.55	0.54	0.70	0.83	1.10	1.35	1.60
	0.8	0.24	0.38	0.52	0.50	0.65	0.77	1.00	1.22	1.43
	0.9	0.23	0.36	0.49	0.47	0.60	0.71	0.92	1.11	1.30
	1.0	0.22	0.35	0.46	0.45	0.57	0.66	0.85	1.02	1.19
	1.1	0.22	0.33	0.44	0.42	0.53	0.62	0.79	0.95	1.09
	1.3	0.21	0.31	0.40	0.39	0.48	0.56	0.70	0.83	0.94
	[23]	0.19		0.40			0.71	1.17	1.85	
	[53]	0.23		0.51			0.71	0.88		
	[37]	0.20		0.48			0.72	0.92		
	[54]	0.24		0.51			0.73	0.93		

[23] → Vinodkumar-1999, [54]→ Gunar-1997 ,[53] → Juan-Luis-2008, [37] → Eichten-1980.

conventional Van Royen-Weisskopf formula for the di-gamma and di-leptonic decay widths. Like in many other theoretical models, we also consider the contribution from the radiative corrections to these decays. Accordingly, the two photon decay width of the pseudoscalar meson is computed as

$$\Gamma_{0^{-+}\to\gamma\gamma} = \Gamma_0 + \Gamma_R \tag{17}$$

where Γ_0 is the conventional Van Royen-Weisskopf formula given by [41]

$$\Gamma_0 = \frac{12\alpha_e^2 e_Q^4}{M_P^2}\ |R_{nS}(0)|^2 \tag{18}$$

Table 10. Average quark Velocity in $Q\bar{Q}$ (Q ϵ b, c) states with various potential power index.

	CPP$_\nu$ ν	1S	1P	2S	1D	2P	3S	4S	5S	6S
$c\bar{c}$:$\langle v_c^2\rangle^{\frac{1}{2}}$	0.7	0.245	0.263	0.268	0.297	0.289	0.295	0.320	0.341	0.360
	0.8	0.265	0.296	0.309	0.343	0.339	0.351	0.388	0.421	0.450
	0.9	0.283	0.329	0.350	0.389	0.391	0.410	0.462	0.509	0.550
	1.0	0.300	0.361	0.392	0.435	0.445	0.472	0.541	0.603	0.660
	1.1	0.316	0.392	0.434	0.480	0.499	0.536	0.625	0.705	0.779
	1.3	0.345	0.451	0.518	0.569	0.610	0.669	0.804	0.928	1.043
	[54]	0.27	0.29	0.35	0.34	0.39	0.44	0.52		
$b\bar{c}$:$\langle v_c^2\rangle^{\frac{1}{2}}$	0.7	0.396	0.419	0.427	0.472	0.459	0.469	0.507	0.540	0.570
	0.8	0.427	0.472	0.492	0.544	0.539	0.558	0.616	0.667	0.713
	0.9	0.457	0.524	0.558	0.617	0.622	0.652	0.733	0.806	0.871
	1.0	0.484	0.575	0.624	0.690	0.706	0.749	0.859	0.956	1.045
	1.1	0.509	0.624	0.691	0.762	0.793	0.851	0.991	1.118	1.234
	1.3	0.555	0.719	0.825	0.904	0.970	1.063	1.276	1.471	1.653
$b\bar{c}$:$\langle v_b^2\rangle^{\frac{1}{2}}$	0.7	0.030	0.032	0.032	0.036	0.035	0.036	0.038	0.041	0.043
	0.8	0.032	0.036	0.037	0.041	0.041	0.042	0.047	0.051	0.054
	0.9	0.035	0.040	0.042	0.047	0.047	0.049	0.056	0.061	0.066
	1.0	0.037	0.044	0.047	0.052	0.054	0.057	0.065	0.073	0.079
	1.1	0.039	0.047	0.052	0.058	0.060	0.065	0.075	0.085	0.094
	1.3	0.042	0.055	0.063	0.069	0.074	0.081	0.097	0.112	0.126
$b\bar{b}$:$\langle v_b^2\rangle^{\frac{1}{2}}$	0.7	0.077	0.074	0.076	0.081	0.079	0.081	0.086	0.092	0.096
	0.8	0.083	0.083	0.087	0.094	0.093	0.096	0.105	0.113	0.121
	0.9	0.088	0.093	0.098	0.106	0.107	0.113	0.125	0.137	0.148
	1.0	0.093	0.101	0.110	0.119	0.122	0.130	0.147	0.163	0.178
	1.1	0.097	0.110	0.122	0.132	0.137	0.147	0.170	0.191	0.210
	1.3	0.105	0.127	0.145	0.157	0.168	0.184	0.220	0.252	0.283
	[53]	0.094		0.091			0.103	0.120		
	[54]	0.080	0.068	0.081	0.075	0.085	0.096	0.112		

[53] →Juan-Luis-2008, [54]→ Gunar-1997.

and Γ_R is the radiative correction given by [25]

$$\Gamma_R = \frac{\alpha_s}{\pi}\left(\frac{\pi^2-20}{3}\right)\Gamma_0 \tag{19}$$

Similarly, the leptonic decay widths of the vector mesons with radiative correction is computed as

$$\Gamma_{1^{--}\to l^+l^-} = \Gamma_{VW} + \Gamma_{rad} \tag{20}$$

Table 11. $0^{-+} \rightarrow \gamma\ \gamma$ decay rates (in ke$V$) of heavy qurkonia states (Bracketed quantities are with QCD corrections).

	CPP$_\nu$	1S	2S	3S	4S	5S	6S
	ν	$\Gamma_0(\Gamma_{\gamma\gamma})$	$\Gamma_0(\Gamma_{\gamma\gamma})$	$\Gamma_0(\Gamma_{\gamma\gamma})$	$\Gamma_0(\Gamma_{\gamma\gamma})$	$\Gamma_0(\Gamma_{\gamma\gamma})$	$\Gamma_0(\Gamma_{\gamma\gamma})$
$c\bar{c}$	0.7	5.87(3.98)	2.83(1.92)	1.92(1.30)	1.47(1.00)	1.20(0.82)	1.02(0.69)
	0.8	6.29(4.26)	3.15(2.13)	2.17(1.47)	1.68(1.14)	1.38(0.93)	1.17(0.80)
	0.9	6.65(4.51)	3.44(2.33)	2.40(1.63)	1.87(1.27)	1.54(1.04)	1.31(0.89)
	1.0	6.98(4.73)	3.70(2.51)	2.61(1.77)	2.03(1.38)	1.68(1.14)	1.43(0.97)
	1.1	7.26(4.92)	3.93(2.67)	2.79(1.89)	2.18(1.48)	1.80(1.22)	1.53(1.04)
	1.3	7.74(5.24)	4.33(2.93)	3.08(2.08)	2.40(1.62)	1.97(1.33)	1.66(1.13)
	[5]	7.2±0.7	1.3 ± 0.6*				
	[55]	7.5 − 10	3.5 − 4.5				
	[56]	7.14±0.95	4.44±0.48				
	[16]	5.5	1.8				
$b\bar{b}$	0.7	0.44(0.33)	0.20(0.15)	0.14(0.11)	0.11(0.08)	0.09(0.07)	0.08(0.06)
	0.8	0.47(0.36)	0.23(0.18)	0.17(0.13)	0.13(0.10)	0.11(0.09)	0.10(0.07)
	0.9	0.50(0.38)	0.26(0.20)	0.19(0.15)	0.16(0.12)	0.13(0.10)	0.12(0.09)
	1.0	0.53(0.40)	0.29(0.22)	0.22(0.17)	0.18(0.14)	0.16(0.12)	0.14(0.11)
	1.1	0.55(0.42)	0.32(0.25)	0.25(0.19)	0.21(0.16)	0.18(0.14)	0.16(0.12)
	1.3	0.60(0.45)	0.38(0.29)	0.31(0.23)	0.26(0.20)	0.23(0.18)	0.21(0.16)
	[55]	0.56	0.269	0.208			
	[56]	0.384±0.047	0.191±0.025				
	[16]	0.35	0.15	0.1			

[5]→ PDG-2006 ,[55] →Lansberg-2008, [56] → Kim-2005,
[16] →Ebert-2003 ,* →Anser-2004 [57].

where Γ_{VW} is the conventional Van Royen-Weisskopf formula given by

$$\Gamma_{VW} = \frac{4\alpha_e^2 e_Q^2}{M_V^2}\ |R_{nS}(0)|^2 \tag{21}$$

and the radiative correction Γ_{rad} is given by

$$\Gamma_{rad} = \ -\frac{16}{3\pi}\alpha_s\ \Gamma_{VW}, \tag{22}$$

It is obvious to note that the computations of the decay rates and the radiative correction terms described here require the right description of the meson state through its radial wave function at the origin R(0) and its mass M which in turn depend on the model parameters like α_s, confinement strength and quark model masses. Generally, due to lack of exact solutions for colour dynamics and with the uncertainties over the exact nature of interquark potential, R(0) and M are also been considered as free parameters of the theory [58]. However, we found it appropriate to employ the spectroscopic parameters of the mesons such as the phenomenologically predicted meson mass and the corresponding wave function predicted by different models for the estimation

Table 12. $1^{--} \rightarrow l^+ l^-$ decay rates (in ke$V$) of heavy qurkonia states (Bracketed quantities are with QCD corrections).

	CPP$_\nu$	1S	2S	3S	4S	5S	6S
	ν	$\Gamma_{VW}(\Gamma_{ll})$	$\Gamma_{VW}(\Gamma_{ll})$	$\Gamma_{VW}(\Gamma_{ll})$	$\Gamma_{VW}(\Gamma_{ll})$	$\Gamma_{VW}(\Gamma_{ll})$	$\Gamma_{VW}(\Gamma_{ll})$
$c\bar{c}$	0.7	5.64(2.77)	2.44(1.20)	1.60(0.79)	1.21(0.59)	0.97(0.48)	0.82(0.40)
	0.8	6.19(3.04)	2.78(1.36)	1.85(0.91)	1.41(0.69)	1.14(0.56)	0.96(0.47)
	0.9	6.69(3.28)	3.12(1.53)	2.10(1.03)	1.61(0.79)	1.30(0.64)	1.10(0.54)
	1.0	7.16(3.51)	3.45(1.69)	2.35(1.15)	1.80(0.88)	1.47(0.72)	1.24(0.61)
	1.1	7.60(3.73)	3.78(1.85)	2.60(1.27)	1.99(0.98)	1.62(0.80)	1.37(0.67)
	1.3	8.38(4.11)	4.41(2.17)	3.07(1.51)	2.37(1.16)	1.92(0.94)	1.62(0.79)
	[5]	5.55±0.14	2.48±0.06	0.86±0.07	0.58±0.07		
	[16]	6.7(5.4)	3.2(2.4)				
$b\bar{b}$	0.7	1.37(0.84)	0.62(0.38)	0.43(0.26)	0.33(0.21)	0.28(0.17)	0.24(0.15)
	0.8	1.47(0.91)	0.71(0.44)	0.51(0.31)	0.41(0.25)	0.34(0.21)	0.30(0.18)
	0.9	1.57(0.97)	0.81(0.50)	0.59(0.37)	0.48(0.30)	0.41(0.25)	0.36(0.22)
	1.0	1.65(1.02)	0.90(0.56)	0.68(0.42)	0.56(0.34)	0.48(0.30)	0.43(0.26)
	1.1	1.74(1.07)	1.00(0.62)	0.77(0.47)	0.64(0.39)	0.56(0.34)	0.50(0.31)
	1.3	1.88(1.16)	1.19(0.74)	0.95(0.59)	0.81(0.50)	0.71(0.44)	0.64(0.40)
	[5]	1.34±0.018	0.612±0.011	0.443±0.008	0.272±0.029	0.31±0.071	0.13±0.03
	[16]	1.4(1.3)	0.6(0.5)				

[5] → PDG2006, [16] → Ebert-2003.

of the decay properties of the mesons.

Making use of the model parameters, the resultant radial wave functions and the mesonic mass we compute the $0^{-+} \rightarrow \gamma\,\gamma$ and $1^{--} \rightarrow l^+\,l^-$ decay widths for each cases of the potential model employed here for the present study. The results are shown in Table (11) for $0^{-+} \rightarrow \gamma\,\gamma$, and in Table (12) for $1^{--} \rightarrow l^+\,l^-$ in comparison with the predictions of the contemporary potential models and with the known experimental values. The bracketed quantities listed in both the tables are the decay widths with the respective radiative corrections added to the conventional V-W formula as per Eqn.17 and Eqn. 20 respectively.

7. Results and Discussion

We have employed the coulomb plus power potential form to study the mass spectrum and decay properties of heavy mesons. Unlike in our earlier studies using variational approach [24, 25], here we solved the Schrödinger equation numerically using [34]. It helps us to study the mass spectrum of $c\bar{c}$, $b\bar{c}$ and $b\bar{b}$ mesons up to few excited states. Our potential parameters are fixed with respect to the centre of weight ground state $1S$ mass of the $Q\bar{Q}$ $(Q\ \epsilon\ b, c)$ systems. Our predication of the excited state of these

mesons for the potential index $\nu = 0.9$ to 1.3 are found to be in good agreement with the experimental results as well as with theoretical predictions of other models. Success of the present study is not only related to the numerical approach but also to the fact that the strength of the confinement part of the potential is made state dependent according to the relation $\frac{A}{(n+1)^{\frac{1}{4}}}$.

In Table 2, we tabulate the values of the S-wave radial wave function at the origin, $|R_{ns}(0)|^2$ (in GeV^3) for the S- wave of heavy $Q\bar{Q}$ systems along with other models. These quantities are not only essential inputs for evaluating decay constants, decay rates, NRQCD parameters and production cross sections for quarkonium states but also important for the determination of hyperfine and fine splitting of their mass spectra. We compared our prediction for the $|R(0)|^2$ with that of Martin potential [7], Logarithmic potential [10], Cornell potential [37], Buchmuller-Tye potential [6] and Lichtenberg-Wills potential [38]. We also observe that a model independent relationship for the radial wave function of the $b\bar{c}$ with that of $c\bar{c}$ and $b\bar{b}$ system as given by [59]

$$|\psi_{b\bar{c}}|^2 \approx |\psi_{c\bar{c}}|^{2(1-q)} \, |\psi_{b\bar{b}}|^{2q} \tag{23}$$

with $q = 0.35$, seem to hold within 2% variation for the lower states in the potential range $0.5 \leq \nu \leq 1.5$ and for higher states we find the relation hold within 5% for all values for ν studied here.

Our results for the decay constant of pseudoscalar meson f_P, vector meson f_V and their ratio of f_P/f_V with and without the QCD corrections (given in brackets) for $c\bar{c}$, $b\bar{c}$ and $b\bar{b}$ mesons are listed in Tables 6 to 8 respectively from $1S$ to $6S$ states. Our results are compared with the available experimental values [5] and with other theoretical predications. We could see that reduction in the f_P values to about 19% in the cases of $c\bar{c}$, 14% in the case of $b\bar{b}$ and 10% in the case of $b\bar{c}$ and reduction in the f_V values to about 25% in the cases of $c\bar{c}$, 19% in the case of $b\bar{b}$ and 16% in the case of $b\bar{c}$ are attributed due to the QCD correction factor. Our results for $1S$ state of f_P for $c\bar{c}$ system is in good agreement with the values reported by CLEO collaboration and f_V with the PDG average value [5]. The ratio f_P/f_V without the QCD correction predicted by us lie between 0.87 to 0.8 in the potential range of $0.7 \leq \nu \leq 1.3$ as against the experimental ratio of 0.81 ± 0.19 [5]. The predicted values of f_P for $2S$ to $6S$ states are in accordance with other theoretical predictions. Our results for the $c\bar{c}$ meson decay constants without the QCD corrections are in good agreement with the experimental data, while that for $b\bar{b}$ system with the QCD corrections are in accordance with the experimental results as well as with other model predictions. The predicted properties of the $b\bar{c}$ system are expected to be supported by the future experimental observations.

In Table 9, we present the mean square radii of $Q\bar{Q}$ (Q ϵ b, c) systems. Our predicted values are in accordance with few available predictions for $c\bar{c}$ and $b\bar{b}$ states available in literature. However for the $b\bar{c}$ system we do not find their sizes available in literature for comparison.

In Table 10, the average quark velocity at the ground state as well as at different excited states $\langle v_q^2 \rangle^{\frac{1}{2}}$ of $Q\bar{Q}$ (Q ϵ b, c) systems are listed for the potential index $\nu = 0.7$ to 1.3.

The present results are in unit of the velocity of light. Our results for $c\bar{c}$ and $b\bar{b}$ systems are in accordance with the existing values reported by others [54]up to $4S$ states. As expected, the quark velocity $\langle v_q^2 \rangle^{\frac{1}{2}}$ increases with higher excited states. However, it is also been observed that with increase in the potential index ν, the quark velocity also increases (See Table 10). It corresponds to strong binding and fast motion unlike the usually expected case of strong binding and slow motion. The predicted quark velocity of $c\bar{c}$ system in $6S$ states for the potential index 1.3 is interesting as it exceeds unity. Probably it may be the indication of the limit at which the $c\bar{c}$ can excite. It is also supported by the fact that there exist little experimental evidence for the higher excited states of $c\bar{c}$ systems beyond $4S$ level. In this potential index of 1.3 the quark velocity approaches the velocity of light from its $4S$ state onwards (0.8c) warranting the relativistic approaches to study this states and beyond. For the choices $\nu < 1.3$, such problems do not seem to be important even up to the $6S$ states.

In the case of $b\bar{b}$ systems up to $6S$ states for all the potential index studied here suggest the validity of nonrelativistic treatment. The b-quark/antiquark velocities up to $6S$ states obtained here for all the choices of the potential index $0.7 \leq \nu \leq 1.3$ lie below $0.3c$. Thus supporting the existence of higher excited states for $b\bar{b}$ system compared to $c\bar{c}$ system observed experimentally. In the case of $b\bar{c}$ system, we have computed the velocity of c-quark as well as that of the b-quark at different excited states. The charm quark in $b\bar{c}$ system seemed to move faster than its counter part in $c\bar{c}$ system, while the b-quark in $b\bar{c}$ system moves slower than that in $b\bar{b}$ system. Also, the importance of relativistic effects to the motion of c-quark is evident for the study of its excited states beyond $2S$ level as per the velocity predictions by the choices of power index above 0.9. This observation in our present study also support the fact that the higher excited levels will be loosely bound and may not be formed to be seen experimentally. Over and above the predicted values of $\langle v_q^2 \rangle^{\frac{1}{2}}$ would be useful in the study of the decay properties of $Q\bar{Q}$ systems using NRQCD formalism.

Our computed values of the di-gamma and leptonic decay widths with and without the radiative corrections are shown in Tables 11 and 12 respectively. Our predictions for $c\bar{c} \rightarrow \gamma\gamma$ are in good agreement with the experimental result for the potential index $\nu = 1.1$ to 1.3, with out the radiative corrections. But, in the case of $b\bar{b} \rightarrow \gamma\gamma$ we find our predictions with the radiative correction are in accordance with the values reported by others [56, 16]. In the case of leptonic decay widths, our predictions Γ_{VW} for both $c\bar{c}$ and $b\bar{b}$ systems are found to be slightly over estimated in the same range of potential index, $1.1 \leq \nu \leq 1.3$ and that with the radiative corrections, Γ_{ll} are under estimated. If may be the indication of the fact that these decay of quarkonia occur not at zero separation of the quark and antiquark but at some finite separation. We must also look into the various aspects of the decay of quarkonia discussed within the NRQCD like formalism. We envisage such attempts for our future works.

We further conclude here that the present study of the properties of $Q\bar{Q}$ $(Q \; \epsilon \; b, c)$ systems based on the non-relativistic coulomb plus power potential with the power index ranging from 0.1 to 1.5 using numerical approach to solve the Schrödinger equation is

an attempt to understand the exact nature of the inter-quark potential and their parameters that provided us the spectroscopic properties as well as the decay properties of the $Q\bar{Q}$ system. We observe that most of the properties of the $Q\bar{Q}$ systems predicted with the potential index in the range of $0.7 \leq \nu \leq 1.3$ are in good agreement with the existing experimental results as well as with other theoretical model predictions.

Acknowledgement: Part of this work is done with a financial support from DST, Government of India, under a MajorResearch Project **SR/S2/HEP-20/2006**. We would like to thank Wolfgang LUCHA (Vienna) and Franz F. Schöberl (Vienna) for providing the Mathematica code of numerical solution of two body Schrödinger equation.

Refrences

[1] N. Brambilla, arXiv:hep-ph/0702105v2.
[2] Kamal K Seth, arXiv:hep-ex/0504050v1.
[3] T. Branes, S. Godfrey and E. S. Swanson, Phys.Rev **D 72**, 054026 (2005),arXiv:hep-ex/0505002v3.
[4] Heavy Quarkonium Physics, N. Brambilla et. al, CERN Yellow Report, CERN-2005-005, Geneva: CERN2005, arXiv:hep-ph/0412158v2.
[5] W. M. Yao et al., (Partcle Data Group) J. Phys.**G 33**, 1 (2006).
[6] Buchmuller and Tye, Phys.Rev **D 24**, 132 (1981).
[7] A. Martin, Phys. Lett. **93 B** 338 (1980).
[8] A. Martin, Phys. Lett. **82 B** 272 (1979).
[9] J. L. Richardson, Phys. Lett. **82 B**, 272 (1979).
[10] C. Quigg and J. L. Rosner, Phys. Lett. 71 B 153(1977).
[11] C. Quigg and J. L. Rosner, Phys. Rept. **56** 167-235 (1979).
[12] E. Eichten et. al., Phys. Rev. **D 17**, 3090 (1978).
[13] Vijaya Kumar K B, B Hanumaiah and S Pepin, Eur.Phys. J. **A 19** 247 (2004).
[14] Altarelli G, Cabibbo N, Corbo G, Maiani L and Martinelli G, Nucl. Phys. **B 208.** 365 (1982).
[15] D. Ebert R.N. Faustov and V. O. Galkin, Phys. Rev **D67** 014027 (2003).
[16] D. Ebert R.N. Faustov and V. O. Galkin, Mod. Phys. Lett **A18** 601 (2003).
[17] J. L. Rosner et al. (CLEO Collaboration), Phys. Rev. Lett.**96**, 092003 (2006).
[18] S. N. Gupta, J. M. Johnson and W. W. Repko, Phys. Rev. **D 54**,2075(1996).
[19] S. Godfrey, Phys. Rev. **D 33**,1391(1986).
[20] S. B. Khadkikar and S. K. Gupta, Phys. Lett. **B 124**, 523(1983).
[21] Hwang D. S., Kim C. S. and Wuk Namgung, Phys. Rev. D **53**, 4951 (1996).
[22] J. N. Pandya and P. C. Vinodkumar, Pramana J. Phys **57**,821 (2001).
[23] P. C. Vinodkumar, J. N. Pandya, V. M. Bannur and S. B. Khadkikar, Eur. Phys. J. **A 4**, 83-90 (1999).
[24] Ajay Kumar Rai, R H Parmar and P C Vinodkumar Jnl. Phys G. **28**,2275-2280 (2002).
[25] Ajay Kumar Rai, J N Pandya and P C Vinodkumar Jnl. Phys G. **31**, 1453 (2005).
[26] Ajay Kumar Rai and P C Vinodkumar, Pramana J. Phys. **66**, 953 (2006).
[27] A. Adb El-Hady, M.A.K. Lodhi and J.P. Vary, Phys. Rev. **D 59** 094001 (1999).
[28] S. F. Radford and W. W. Repko, Phys. Rev. **D 75**, 074031 (2007).
[29] Chin-Wen Hwang and Zheng-Tao Wei, J. Phys.**G 34**, 687 (2007), hep-ph/0609036.
[30] H. Y. Cheng, C. Y. Cheung and C. W. Hwang, Phys. Rev. **D 55**, 1159 (1997).
[31] Sameer M. Ikhdair et. al, Int. Jn. Mod. Phys. **A 19**, 1771 (2004), *ibid* **A 20**, 4035 (2005).

[32] L. Motyka and K. Zalewiski, Eur. Phys. J. **C 4** 107 (1998); *ibid.*, Z. Phys. **C 69** , 343 (1996).
[33] X. T. Song, J. Phys. **G 17**, 49 (1991).
[34] W. Lucha and F Schoberl, Int. J. Mod. Phys. **C 10** 607 (1999), arXiv:hep-ph/9811453v2.
[35] Gershtein S S, Kiselev V V, Likhoded A K and Tkabladze A V, Phys. Rev. **D 51**, 3613 (1995).
[36] N. Brambilla, Y. Sumino and A. Vairo ,Phys. Rev **D 65** 034001 (2002). arXiv:hep-ph/0108084.
[37] E. J. Eichten,K. Gotfried, T. Kinoshita, K. Lane, T. Yan, Phys. Rev. **D 21**, 203 (1980).
[38] D. B. Lichenberg and J. G. Wills, Nuovo Cimento **A 47**, 483 (1978).
[39] J. Zeng, J. W. Van Orden and W. Roberts, Phys. Rev. **D 52**,5229 (1995).
[40] A. Abd El-Hady. J. R. Spence and J. P. Vary, Phys. Rev **D71**, 034006(2005).
[41] R. Van Royen and V. F. Weisskopf, Nuovo Cimento **50**, (1967).
[42] Bodwin G T, Lee J. and Sinclair D K, Phys. Rev. **D 72** 014009 (2005).
[43] D. S. Hwang and Gwang-Hee Kim, Z. Phys. **C 76** 107 (1997).
[44] Guo-Li Wang. Phys. Lett **B 633**,492-496 (2006).
[45] E. Braaten and S. Fleming, Phys. Rev. **D 52** 181 (1995).
[46] K. W. Edwards et al., CLEO Collabration, Phys. Rev. Lett. **86**, 30 (2001).
[47] G.Cvetic et al., Phys. Lett. **B 596**, 84 (2004).
[48] K. Gottfried, Phys. Rev. Lett. **40**, 598 (1978).
[49] M . B. Voloshin, Nucl. Phys. **B 154**, 365 (1979).
[50] Kuang Y.P and Yan T. M ,Phys. Rev. **D 41**, 155 (1990).
[51] G. T. Bodwin et. al, Phys. Rev. **D 77**, 094017 (2008).
[52] Eichten E J and Quigg, Phys. Rev. **D 49**, 5845(1994).
[53] Juan-Luis Domenesh-Garret and Miguel- Angel Sanchis-Lozano, arXiv:hep-ph/0805.2916v2.
[54] Gunnar S. Bali,Klaus Schilling and Armin Wachter, Phys. Rev. **D 56**, 2566 (1997).
[55] J. P. Lansberg and T. N. Pham, Phys. Rev. **D74**, 034001 (2006) , Phys. Rev. **D75**,017501 (2007), arXiv:hep-ph/0804.2180v1.
[56] C. S. Kim, T. Lee and G. L. Wang, Phys. Lett. **B 606**,323(2005),arXiv:hep-ph/0411075.
[57] D. M. Anser et. al (CLEO Collobaration), Phys. Rev. Lett **92**,142001 (2004).
[58] Hafsakhan and Pervez Hoodbhoy, Phys. Rev. **D53**,2534 (1996).
[59] Sterrett J. Collins, T.D. Imbo, B. A. King, E. C. Martell, Phys. Lett. **B 393** 155-160 (1997).